

Dual-resonance converse magnetoelectric and voltage step-up effects in laminated composite of long-type $0.71\text{Pb}(\text{Mg}_{1/3}\text{Nb}_{2/3})\text{O}_3-0.29\text{PbTiO}_3$ piezoelectric single-crystal transformer and $\text{Tb}_{0.3}\text{Dy}_{0.7}\text{Fe}_{1.92}$ magnetostrictive alloy bars

Chung Ming Leung, Siu Wing Or, Feifei Wang, and S. L. Ho

Citation: *J. Appl. Phys.* **109**, 104103 (2011); doi: 10.1063/1.3587574

View online: <http://dx.doi.org/10.1063/1.3587574>

View Table of Contents: <http://jap.aip.org/resource/1/JAPIAU/v109/i10>

Published by the [American Institute of Physics](#).

Related Articles

Electrostatic tuning of ferromagnetic resonance and magnetoelectric interactions in ferrite-piezoelectric heterostructures grown by chemical vapor deposition
Appl. Phys. Lett. **99**, 192502 (2011)

A four-state magnetoelectric coupling for embedded piezoelectric/magnetic composites
J. Appl. Phys. **110**, 084109 (2011)

Relaxor behavior in multiferroic BiMn_2O_5 ceramics
J. Appl. Phys. **110**, 084101 (2011)

Rietveld analysis, dielectric and magnetic properties of Sr and Ti codoped BiFeO_3 multiferroic
J. Appl. Phys. **110**, 073909 (2011)

Spin-flop driven magneto-dielectric effect in $\text{Co}_4\text{Nb}_2\text{O}_9$
Appl. Phys. Lett. **99**, 132906 (2011)

Additional information on *J. Appl. Phys.*

Journal Homepage: <http://jap.aip.org/>

Journal Information: http://jap.aip.org/about/about_the_journal

Top downloads: http://jap.aip.org/features/most_downloaded

Information for Authors: <http://jap.aip.org/authors>

ADVERTISEMENT

**AIPAdvances**

Submit Now

**Explore AIP's new
open-access journal**

- **Article-level metrics
now available**
- **Join the conversation!
Rate & comment on articles**

Dual-resonance converse magnetoelectric and voltage step-up effects in laminated composite of long-type $0.71\text{Pb}(\text{Mg}_{1/3}\text{Nb}_{2/3})\text{O}_3-0.29\text{PbTiO}_3$ piezoelectric single-crystal transformer and $\text{Tb}_{0.3}\text{Dy}_{0.7}\text{Fe}_{1.92}$ magnetostrictive alloy bars

Chung Ming Leung,¹ Siu Wing Or,^{1,a)} Feifei Wang,² and S. L. Ho¹

¹*Department of Electrical Engineering, The Hong Kong Polytechnic University, Hung Hom, Kowloon, Hong Kong*

²*Key Laboratory of Optoelectronic Material and Device, Mathematics and Science College, Shanghai Normal University, Shanghai 200234, China*

(Received 16 August 2010; accepted 9 April 2011; published online 16 May 2011)

We report a dual-resonance converse magnetoelectric effect and a dual-resonance voltage step-up effect in a laminated composite made by sandwiching the output (or secondary) section of a long-type $0.71\text{Pb}(\text{Mg}_{1/3}\text{Nb}_{2/3})\text{O}_3-0.29\text{PbTiO}_3$ (PMN-PT) piezoelectric single-crystal transformer having a longitudinal-longitudinal polarization between two $\text{Tb}_{0.3}\text{Dy}_{0.7}\text{Fe}_{1.92}$ (Terfenol-D) magnetostrictive alloy bars having a longitudinal magnetization. The reported converse magnetoelectric effect originates from the mechanically mediated resonance converse piezoelectric effect in the PMN-PT transformer and resonance converse magnetostrictive effect in the Terfenol-D bars. The additional voltage step-up effect results from the mechanically mediated resonance converse and direct piezoelectric effects in the PMN-PT transformer. The composite shows two sharp resonance peaks of 0.39 and 0.54 G/V in converse magnetoelectric coefficient ($\alpha_B = dB/dV_{in}$) and of 1.4 and 2.1 in voltage step-up ratio (V_{out}/V_{in}) at about 54 and 120 kHz, corresponding to the half- and full-wavelength longitudinal mode resonances, respectively. The measured magnetic induction (B) exhibits good linear relationships to the applied ac voltage (V_{in}) with amplitude varying from 10 to 100 V in both resonance and nonresonance conditions. These dual-resonance effects make the composite great promise for coil-free electromagnetic device applications. © 2011 American Institute of Physics. [doi:10.1063/1.3587574]

I. INTRODUCTION

The direct magnetoelectric (DME) effect, as proposed by Pierre Curie, is an induced electric polarization in a material by an applied magnetic field, while the converse magnetoelectric (CME) effect, also proposed by Curie, is an induced magnetization in the material by an applied electric field.¹ Since the first observation of the DME and CME effects in Cr_2O_3 antiferromagnetic single crystal in the early 1960s,² a variety of ME materials have been discovered or developed for potential applications in power-free magnetic field/electric current sensors or ME transducers based on the DME effect.³⁻¹⁶ These materials can generally be classified as single-phase and multiphase materials. Single-phase materials have both ferroelectric order and ferromagnetic (or antiferromagnetic) order in the same phase, thus enabling an electric field switchable spontaneous polarization, a magnetic field switchable spontaneous magnetization, and often some coupling between the two.³⁻⁵ However, the weak ME coupling and great challenge to synthesis have greatly limited the practical viability of the single-phase materials. Accordingly, considerable research efforts have been put on multiphase materials in the recent decade, especially on magnetostrictive-piezoelectric laminated composites.⁶⁻¹¹

Today, it is known that laminated composites based on $\text{Tb}_{0.3}\text{Dy}_{0.7}\text{Fe}_{1.92}$ (Terfenol-D) magnetostrictive alloy and $0.71\text{Pb}(\text{Mg}_{1/3}\text{Nb}_{2/3})\text{O}_3-0.29\text{PbTiO}_3$ (PMN-PT) piezoelectric single crystal possess much higher DME effect than those of the others.¹⁰ On the other hand, some specific multilayer composites have been developed, and their DME resonance characteristics have been studied under the influence of magnetic fields.¹²⁻¹⁶

Compared to the DME effect, studies on the CME effect are obviously few, especially on the resonance CME effect. In fact, developing a laminated composite showing a high CME effect is an increasingly important topic for promoting coil-free electromagnetism and the related device physics.¹⁷⁻²⁰ For these reasons, we have developed a laminated composite consisting of a long-type longitudinally-longitudinally polarized PMN-PT piezoelectric single-crystal transformer with its output (or secondary) section sandwiched by two longitudinally magnetized Terfenol-D magnetostrictive alloy bars so as to realize a dual-resonance CME effect through the mechanically mediated resonance converse piezoelectric effect in the PMN-PT transformer and resonance converse magnetostrictive effect in the Terfenol-D bars. Besides, an additional dual-resonance voltage step-up (VSU) effect caused by the mechanically mediated resonance converse and direct piezoelectric effects in the PMN-PT transformer is observed between the output and input (or primary) sections of the PMN-PT transformer in the laminated composite. In fact, the

^{a)}Author to whom correspondence should be addressed. Electronic mail: eeswor@polyu.edu.hk.

use of a piezoelectric transformer instead of a piezoelectric bar/plate is to enable the dual-resonance CME and VSU effects in a single laminated composite. Moreover, the use of this specifically designed long-type piezoelectric transformer (with a longitudinal-longitudinal polarization) in opposition to the traditional Rosen-type piezoelectric transformer (with a transverse-longitudinal polarization) is mainly attributed to the relatively simple structure, ease of impartation of two polarizations of the same direction for the input and output sections, and pure longitudinal mode of operation.

II. STRUCTURE AND OPERATING PRINCIPLE

Figure 1 shows the schematic diagram and photograph of the proposed laminated composite based on a long-type PMN–PT transformer and two Terfenol-D bars. The PMN–PT transformer, with dimensions of 16 (length) \times 2 (width) \times 2 (height) mm³ and having its $\langle 001 \rangle$ crystallographic axis oriented along the longitudinal (or 3-) direction, was cut from a PMN–PT ingot grown in-house by a modified Bridgman method.^{21,22} The as-prepared PMN–PT transformer was painted with silver paste on the two main end surfaces of 2 \times 2 mm² area normal to the longitudinal direction to form the input (or primary) and output (or secondary) electrodes as well as on all the four surfaces covering the central portion of 2 mm length normal to the transverse (or 1-, 2-) directions to form the ground electrode. After firing the silver paste electrodes at 650 °C for 1 h, the PMN–PT transformer was immersed in a silicon oil bath and polarized along its longitudinal direction for both the input and output sections under a dc voltage of 4 kV at 115 °C for 15 min and then under a reduced voltage of 2 kV in a natural cooling run to room temperature. The Terfenol-D bars, with dimensions of 6 mm (length) \times 2 mm (width) \times 2 mm (height) mm³ and having the highly magnetostrictive [112] crystallographic axis oriented along the longitudinal direction, were commercially acquired (Baotou Rate Earth Research Institute, China). To fabricate the laminated composite as shown in

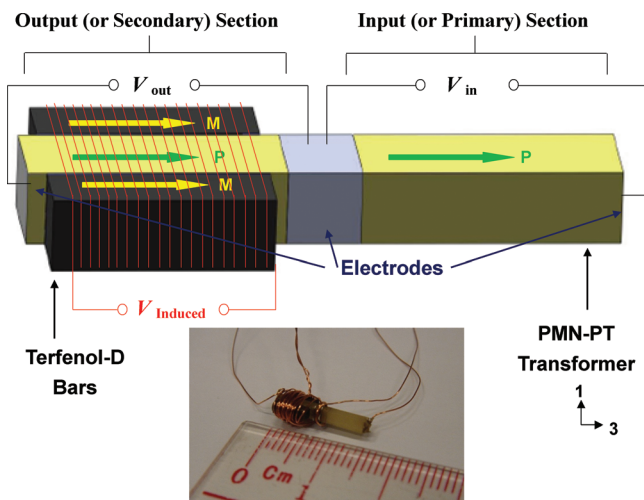


FIG. 1. (Color online) Schematic diagram and photograph of the proposed laminated composite based on a long-type PMN–PT transformer and two Terfenol-D bars. The arrows P denote the electric polarization direction of the PMN–PT transformer, while M indicates the magnetization directions of the Terfenol-D bars.

Fig. 1, the Terfenol-D bars were cleaned by ethanol before being adhered to the output section of the PMN–PT transformer using a nonconductive adhesive and pressed at 8 MPa while cured at 40 °C for 6 h to achieve good mechanical bonding.

The dual-resonance CME effect in our laminated composite is essentially based on the mechanically mediated product effect of the resonance converse piezoelectric effect in the PMN–PT transformer and the resonance converse magnetostrictive effect in the Terfenol-D bars. In more details, an ac voltage (V_{in}) applied to the input section along the longitudinal direction of the PMN–PT transformer leads to longitudinal vibrations due to the converse piezoelectric effect. These longitudinal vibrations, under resonance conditions, are effectively amplified and coupled to the Terfenol-D bars, causing them to produce magnetic induction (B) along their longitudinal direction owing to the converse magnetostrictive effect. As the PMN–PT transformer has a symmetric configuration with a longitudinal-longitudinal polarization in its input and output sections, the laminated composite has two principal CME resonances, corresponding to the half-wavelength ($\lambda/2$) and full-wavelength (λ) longitudinal mode resonances. This is the so-called dual-resonance CME effect in our laminated composite.

In addition to the dual-resonance CME effect, our laminated composite has a simultaneous dual-resonance VSU effect resulting from the mechanically mediated product effect of the resonance converse and direct piezoelectric effects in the PMN–PT transformer. In other words, the amplified longitudinal vibrations associated with the output section of the PMN–PT transformer leads to an enhanced ac voltage in the output section (V_{out}) along the longitudinal direction as a result of the resonance direct piezoelectric effect. Because of the symmetric configuration and longitudinal-longitudinal polarization of the PMN–PT transformer, the PMN–PT transformer with the Terfenol-D bars as the load possesses two main piezoelectric resonances, reflecting the $\lambda/2$ and λ longitudinal mode resonances of the PMN–PT transformer loaded by two Terfenol-D bars. This is said to be the dual-resonance VSU effect in our laminated composite.

III. MEASUREMENTS

The CME effect in the laminated composite was characterized using an in-house automated measurement system as shown in Fig. 2.¹⁷ To acquire the induced magnetic induction (B), a search coil with 30-turn Cu wire of 0.2 mm diameter was wrapped around the output section of the laminated composite, and the whole composite-search coil assembly was placed between the pole gap of a water-cooled, U-shaped electromagnet (Myltem PEM-8005 K). By energizing the electromagnet with a dc current supply (Sorensen DHP200-15), a magnetic bias field (H_{Bias}) of 20–1200 Oe was generated in the pole gap and was measured with a Hall-effect probe connected to a Gaussmeter (F. W. Bell 7030). An arbitrary waveform generator (Agilent 33 210 A) connected to a constant-voltage supply amplifier (AE Techron 7796HF) was employed to provide an applied ac voltage (V_{in}) of 10–100 V peak over the prescribed frequency (f)

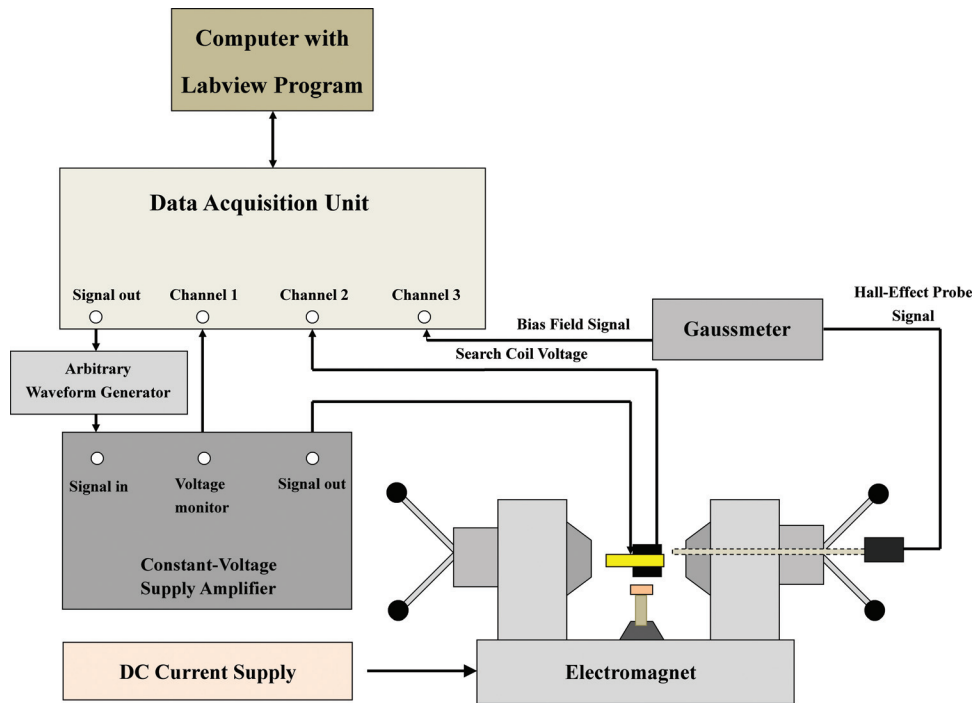


FIG. 2. (Color online) Schematic diagram of the setup for CME measurement.

range of 1–175 kHz to the input section of the laminated composite (i.e., the input section of the PMN–PT transformer). The change in magnetic flux due to V_{in} led to an induced voltage ($V_{Induced}$) in the search coil (Fig. 1). By integrating $V_{Induced}$ with respect to time, the corresponding B induced in the Terfenol-D bars was measured by a data acquisition unit (Nation Instruments BNC-2110 and NI-PCI6132) under the control of a computer with a Labview program.

The VSU effect in the laminated composite was evaluated by measuring the VSU ratio (V_{out}/V_{in}) associated with the output and input sections of the PMN–PT transformer. The arbitrary waveform generator and the constant-voltage supply amplifier were utilized to provide an applied ac voltage (V_{in}) of 100 mV peak and at various frequencies (f) of 1–175 kHz to the input section of the PMN–PT transformer. The data acquisition unit and the computer driven by the Labview program were used to gather the output ac voltage (V_{out}) from the output section of the PMN–PT transformer.

IV. RESULTS AND DISCUSSION

Figure 3 shows the VSU ratio (V_{out}/V_{in}) as a function of frequency (f) for the PMN–PT transformer before and after bonding with the Terfenol-D bars under an applied ac voltage (V_{in}) of 100 mV peak. For the monolithic PMN–PT transformer in Fig. 3(a), two giant sharp resonance peaks are observed at 60 and 122 kHz with different V_{out}/V_{in} values of 28 and 29, respectively. Physically, these two resonance peaks represent the $\lambda/2$ and λ longitudinal mode resonances of the PMN–PT transformer, respectively, as a result of the symmetric configuration with a longitudinal-longitudinal polarization in its input and output sections (Fig. 1). After bonding the Terfenol-D bars onto the output section of the

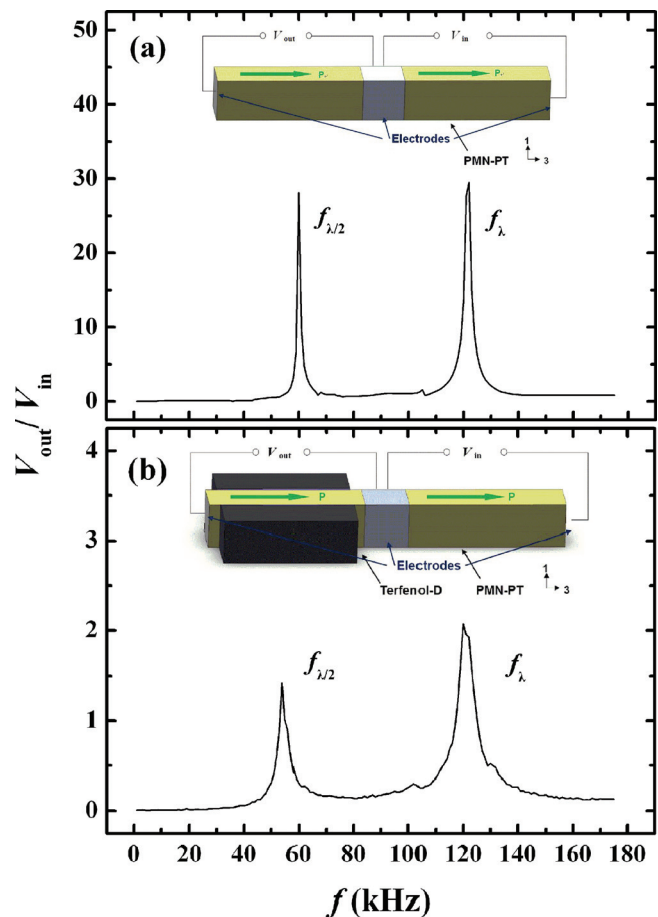


FIG. 3. (Color online) VSU ratio (V_{out}/V_{in}) as a function of frequency (f) for PMN–PT transformer (a) before and (b) after bonding with Terfenol-D bars under an applied ac voltage (V_{in}) of 100 mV peak. The labels $f_{\lambda/2}$ and f_{λ} indicate the half-wavelength ($\lambda/2$) and full-wavelength (λ) longitudinal mode resonance frequencies, respectively.

monolithic PMN-PT transformer in Fig. 3(b), the two resonance peaks as detected in Fig. 3(a) exhibit a reduction in V_{out}/V_{in} to 1.4 and 2.1, together with a shift in resonance frequencies (i.e., $f_{\lambda/2}$ and f_{λ}) to 54 and 120 kHz, respectively, due to the loading effect of the Terfenol-D bars.¹⁶ From another viewpoint, our laminated composite is rather simple in that it is essentially a PMN-PT transformer loaded by two Terfenol-D bars.

Figure 4(a) plots the CME coefficient (α_B) of the laminated composite in the frequency (f) range of 1–175 kHz under various magnetic bias fields (H_{Bias}) of 20–1200 Oe at an applied ac voltage (V_{in}) of 10 V peak. Similar to Fig. 3(b), two obvious resonance peaks in α_B are seen at about 53 and 121 kHz for each H_{Bias} , corresponding to the $\lambda/2$ and λ longitudinal mode resonances of the laminated composite, respectively. In fact, these two resonance α_B have strong dependence on H_{Bias} ; that is, they are maximized with reasonably high values of 0.38 and 0.54 G/V at the minimal $f_{\lambda/2}$ of 53 kHz and f_{λ} of 121 kHz, respectively, when H_{Bias} is set at 800 Oe. This H_{Bias} -induced maximization of α_B and minimization of $f_{\lambda/2}$ and f_{λ} at 800 Oe can be explained by the H_{Bias} -induced maximization of non-180° domain wall motion in the Terfenol-D bars of the laminated composite at shape resonance²³ and will be further discussed in Fig. 5. The reason why the λ longitudinal mode resonance at 121 kHz is stronger than the $\lambda/2$ longitudinal mode resonance at 53 kHz can be ascribed by the longitudinal stress concentration-enhanced CME coupling in the laminated composite via

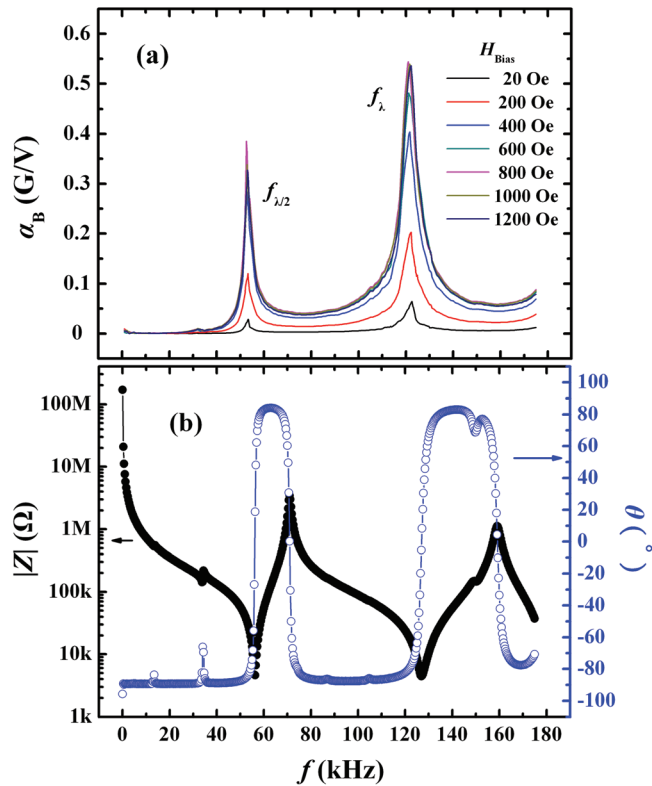


FIG. 4. (Color online) (a) CME coefficient (α_B) of laminated composite in the frequency (f) range of 1–175 kHz under various magnetic bias fields (H_{Bias}) of 20–1200 Oe at an applied ac voltage (V_{in}) of 10 V peak. (b) Electrical impedance ($|Z|$) and phase angle (θ) spectra of laminated composite measured using an impedance analyzer (Agilent 4294 A).

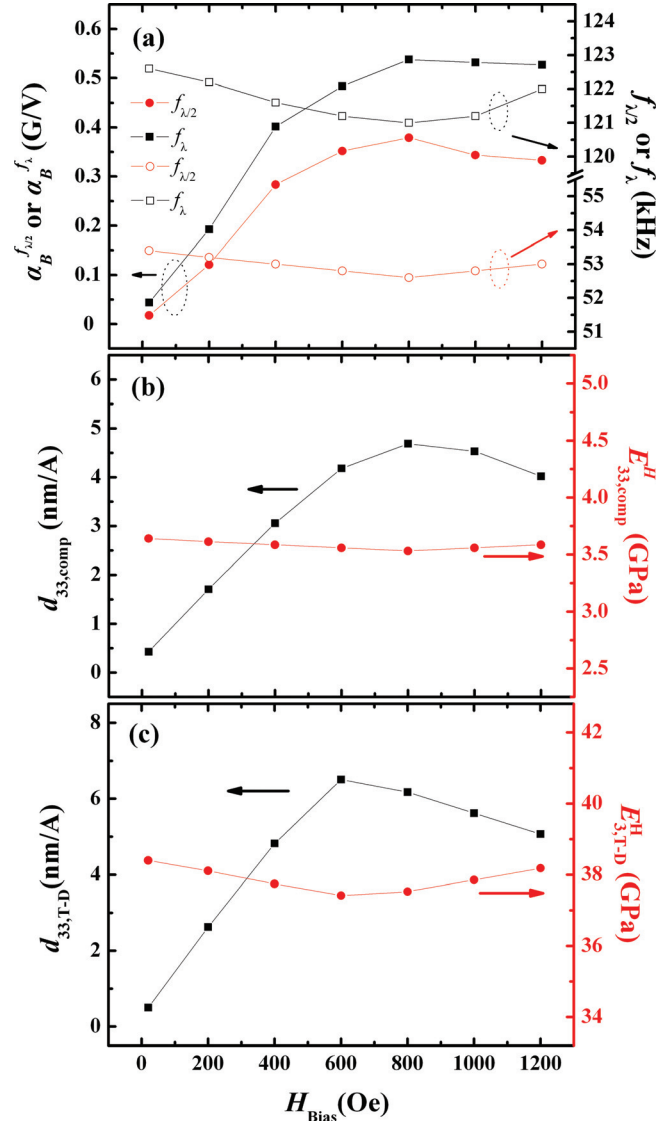


FIG. 5. (Color online) (a) Magnetic bias field (H_{Bias}) dependence of resonance CME coefficients ($\alpha_B^{f_{\lambda/2}}$ and $\alpha_B^{f_{\lambda}}$) for laminated composite at the half-wavelength ($\lambda/2$) and full-wavelength (λ) longitudinal mode resonance frequencies ($f_{\lambda/2}$ and f_{λ}), together with $f_{\lambda/2}$ and f_{λ} . (b) H_{Bias} dependence of piezomagnetic coefficient ($d_{33,comp}^H$) and Young’s modulus at constant magnetic field strength ($E_{33,comp}^H$) of Terfenol-D bars in laminated composite. (c) H_{Bias} dependence of piezomagnetic coefficient ($d_{33,T-D}^H$) and Young’s modulus at constant magnetic field strength ($E_{33,T-D}^H$) of Terfenol-D bars.

an appropriate positioning of the longitudinal vibration nodes at about the centers of the output and input sections of the laminated composite (Fig. 1).²⁴ Figure 4(b) illustrates the electrical impedance ($|Z|$) and phase angle (θ) spectra of the laminated composite measured using an impedance analyzer (Agilent 4294 A). Two clear electromechanical resonances (with minimal $|Z|$ values) are detected at about 53 and 121 kHz, which agree well with the two CME resonances in Fig. 4(a).

In order to give a physical insight into the observed H_{Bias} -induced maximization of α_B and minimization of $f_{\lambda/2}$ and f_{λ} at 800 Oe associated with the CME resonances in Fig. 4(a), Fig. 5(a) shows the magnetic bias field (H_{Bias}) dependence of resonance CME coefficients ($\alpha_B^{f_{\lambda/2}}$ and $\alpha_B^{f_{\lambda}}$) of the laminated composite at the half-wavelength ($\lambda/2$) and

full-wavelength (λ) longitudinal mode resonance frequencies ($f_{\lambda/2}$ and f_λ), together with $f_{\lambda/2}$ and f_λ . The values of $\alpha^{f_{\lambda/2}_B}$, $\alpha^{f_\lambda_B}$, $f_{\lambda/2}$, and f_λ are extracted from Fig. 4(a). It is clear that $\alpha^{f_\lambda_B}$ not only is larger than $\alpha^{f_{\lambda/2}_B}$, but also appears at higher frequencies than $\alpha^{f_{\lambda/2}_B}$. Moreover, $\alpha^{f_{\lambda/2}_B}$ and $\alpha^{f_\lambda_B}$ increase initially with an increase in H_{Bias} , reach their respective maximum values of 0.38 and 0.54 G/V at $H_{\text{Bias}} = 800$ Oe, and then decrease with a further increase in H_{Bias} . At the same time, $f_{\lambda/2}$ and f_λ decrease with increasing H_{Bias} , reaching their respective minimum values of 53 and 121 kHz at $H_{\text{Bias}} = 800$ Oe and then increasing with increasing H_{Bias} . Physically, the initial increase in $\alpha^{f_{\lambda/2}_B}$ and $\alpha^{f_\lambda_B}$ and the corresponding decrease in $f_{\lambda/2}$ and f_λ with increasing H_{Bias} can be explained by the H_{Bias} -induced motion of the available non-180° domain walls in the Terfenol-D bars of the laminated composite at shape resonance.²³ As H_{Bias} is increased near 800 Oe, the compliance associated with increased deformation contribution from this non-180° domain-wall motion is maximized, resulting in a maximum in strain (and hence $\alpha^{f_{\lambda/2}_B}$ and $\alpha^{f_\lambda_B}$) and a minimum in stiffness (and hence $f_{\lambda/2}$ and f_λ). Beyond this critical H_{Bias} level, constraining of non-180° domain-wall motion due to interaction with H_{Bias} gives rise to a decrease in strain (and hence $\alpha^{f_{\lambda/2}_B}$ and $\alpha^{f_\lambda_B}$) and an increase in stiffness (and hence $f_{\lambda/2}$ and f_λ).

To support our discussion, Fig. 5(b) illustrates the magnetic bias field (H_{Bias}) dependence of piezomagnetic coefficient ($d_{33,\text{comp}}$) and Young's modulus at constant magnetic field strength ($E^H_{33,\text{comp}}$) for the Terfenol-D bars in the laminated composite. It is obvious that $d_{33,\text{comp}}$ and $E^H_{33,\text{comp}}$ exhibit similar quantitative trends with resonance α_B and resonance f as shown in Fig. 5(a). This is a result of increasing and maximizing strain (or compliance) contribution from the non-180° domain-wall motion, respectively. In particular, the occurrence of maximum $d_{33,\text{comp}}$ and minimum $E^H_{33,\text{comp}}$ at $H_{\text{Bias}} = 800$ Oe suggests that the Terfenol-D bars in the laminated composite is preferably biased in such a way that the strain (or compliance) associated with increased deformation contribution from this non-180° domain-wall motion is maximized, leading to a maximum in $d_{33,\text{comp}}$ and a minimum in $E^H_{33,\text{comp}}$.^{23,25} Above this critical H_{Bias} level, the decrease in $d_{33,\text{comp}}$ and increase in $E^H_{33,\text{comp}}$ with increasing H_{Bias} are characterized by constraining of non-180° domain-wall motion caused by domain saturation where strain (or compliance) remains essentially constant with increasing H_{Bias} .^{23,25} To further support our discussion, Fig. 5(c) plots the magnetic bias field (H_{Bias}) dependence of piezomagnetic coefficient ($d_{33,\text{T-D}}$) and Young's modulus at constant magnetic field strength ($E^H_{33,\text{T-D}}$) of a Terfenol-D bar used in the laminated composite. It is noted that $d_{33,\text{T-D}}$ and $E^H_{33,\text{T-D}}$ are quantitatively similar to $d_{33,\text{comp}}$ and $E^H_{33,\text{comp}}$ in Fig. 5(b) as well as to resonance α_B and resonance f in Fig. 5(a), respectively. A shift in the critical H_{Bias} from 800 to 600 Oe is due to the load-free condition of the Terfenol-D bar under test.

Figure 6 plots the dependence of applied ac voltage (V_{in}) on magnetic induction (B) at an optimal magnetic bias field (H_{Bias}) of 800 Oe at the half-wavelength ($\lambda/2$) longitudinal mode resonance frequency ($f_{\lambda/2}$), full-wavelength (λ) longitudinal mode resonance frequency (f_λ), and nonresonance

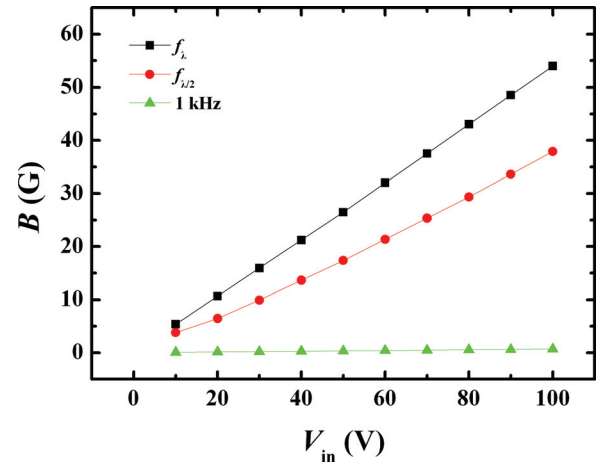


FIG. 6. (Color online) Dependence of applied ac voltage (V_{in}) on magnetic induction (B) at an optimal magnetic bias field (H_{Bias}) of 800 Oe at the half-wavelength ($\lambda/2$) longitudinal mode resonance frequency ($f_{\lambda/2}$), full-wavelength (λ) longitudinal mode resonance frequency (f_λ), and nonresonance frequency of 1 kHz.

frequency of 1 kHz. For all cases, B demonstrates a good linear response to V_{in} in the entire V_{in} range of 10–100 V peak. From the slope of the plots, $\alpha^{f_{\lambda/2}_B}$, $\alpha^{f_\lambda_B}$, and $\alpha_B = 1$ kHz are determined to be 0.38, 0.54, and 0.071 G/V, respectively.

V. CONCLUSION

We have fabricated a laminated composite based on a specific combination of a long-type PMN–PT transformer and two Terfenol-D bars, and investigated its dual-resonance CME and VSU effects. It has been found from the α_B and $V_{\text{out}}/V_{\text{in}}$ spectra that there are two sharp resonance peaks at about 53 and 121 kHz in the laminated composite, corresponding to the $\lambda/2$ and λ longitudinal mode resonances, respectively. Moreover, the two resonance α_B are 0.38 and 0.54 G/V at an optimal H_{Bias} of 800 Oe, while the two resonance $V_{\text{out}}/V_{\text{in}}$ are 1.4 and 2.1, respectively. The dual-resonance CME effect has been attributed to the mechanically mediated resonance converse piezoelectric effect in the PMN–PT transformer and resonance converse magnetostrictive effect in the Terfenol-D bars, while the dual-resonance VSU effect has been ascribed to the mechanically mediated resonance converse and direct piezoelectric effects in the PMN–PT transformer. These dual-resonance CME and VSU effects not only promote coil-free electromagnetism, but also coil-free electromagnetic device applications.

ACKNOWLEDGMENTS

This work was supported by the Research Grants Council of the HKSAR Government (Grant No. PolyU 5266/08E), The Hong Kong Polytechnic University (Grant Nos. 1-ZV7P and 4-ZZ7 T), the Science and Technology Commission of Shanghai Municipality (Grant No. 10ZR1422300), and the Innovation Program of Shanghai Municipal Education Commission (Grant No. 11YZ82).

¹P. Curie, J. Phy. **3**, 393 (1894).

²D. N. Astrov, Sov. Phys. **11**, 708 (1960).

- ³G. L. Yuan, K. Z. Baba Kishi, J. M. Liu, S. W. Or, Y. P. Wang, and Z. G. Liu, *J. Am. Ceram. Soc.* **89**, 3136 (2006).
- ⁴G. L. Yuan, S. W. Or, H. L. W. Chan, and Z. G. Liu, *J. Appl. Phys.* **101**, 024106 (2007).
- ⁵G. L. Yuan, S. W. Or, and H. L. W. Chan, *J. Appl. Phys.* **101**, 064101 (2007).
- ⁶J. Ryu, A. V. Carazo, K. Uchino, and H. E. Kim, *Jpn. J. Appl. Phys.* **40**, 4948 (2001).
- ⁷S. X. Dong, J. F. Li, and D. Viehland, *Appl. Phys. Lett.* **85**, 5305 (2004).
- ⁸S. S. Guo, S. G. Lu, Z. Xu, X. Z. Zhao, and S. W. Or, *Appl. Phys. Lett.* **88**, 182906 (2006).
- ⁹C. M. Chang and G. P. Carman, *J. Appl. Phys.* **102**, 124901 (2007).
- ¹⁰Y. J. Wang, S. W. Or, H. L. W. Chan, X. Y. Zhao, and H. S. Luo, *J. Appl. Phys.* **103**, 124511 (2008).
- ¹¹C. M. Leung, S. W. Or, S. Y. Zhang, and S. L. Ho, *J. Appl. Phys.* **107**, 09D918 (2010).
- ¹²R. Islam and H. Kim, *Appl. Phys. Lett.* **89**, 152908 (2006).
- ¹³Y. K. Fetisov, A. A. Bush, K. E. Kamentsev, A. Ostashenko, and G. Srinivasan, *IEEE Sens. J.* **6**, 935 (2006).
- ¹⁴M. Karmarkar, S. Dong, J. Li, D. Viehland, and S. Priya, *Phys. Status Solidi (RRL)* **2**, 108 (2008).
- ¹⁵D. A. Pan, Y. Bai, A. A. Volinsky, W. Y. Chu, and L. J. Qiao, *Appl. Phys. Lett.* **92**, 052904 (2008).
- ¹⁶Y. J. Wang, C. M. Leung, F. F. Wang, S. W. Or, X. Y. Zhao, and H. S. Luo, *J. Phys. D.: Appl. Phys.* **42**, 135414 (2009).
- ¹⁷Y. M. Jia, S. W. Or, H. L. W. Chan, X. Y. Zhao, and H. S. Luo, *Appl. Phys. Lett.* **88**, 242902 (2006).
- ¹⁸M. Bibes and A. Barthélémy, *Nat. Mater.* **7**, 425 (2008).
- ¹⁹Y. J. Wang, F. F. Wang, S. W. Or, H. L. W. Chan, X. Y. Zhao, and H. S. Luo, *Appl. Phys. Lett.* **93**, 113503 (2008).
- ²⁰Y. M. Jia, F. F. Wang, X. Y. Zhao, H. S. Luo, S. W. Or, and H. L. W. Chan, *Compos. Sci. Technol.* **68**, 1440 (2008).
- ²¹H. S. Luo, G. S. Xu, H. Q. Xu, P. C. Wang, and Z. W. Yin, *Jpn. J. Appl. Phys.* **39**, 5581 (2000).
- ²²F. F. Wang, W. Z. Shi, Y. X. Tang, X. M. Chen, T. Wang, and H. S. Luo, *Appl. Phys. A* **100**, 1231 (2010).
- ²³S. W. Or, T. Li, and H. L. W. Chan, *J. Appl. Phys.* **97**, 10M308 (2005).
- ²⁴Y. H. Jeong, S. H. Lee, J. H. Yoo, and C. Y. Park, *Sens. Actuat.* **77**, 126 (1999).
- ²⁵G. Engdahl, *Handbook of Giant Magnetostrictive Materials* (Academic, San Diego, 2002).